Modulation of Spacing and Magnetic Properties of Iron Oxide Nanoparticles through Polymer-Mediated "Bricks and Mortar" Self-assembly

Andrew K. Boal,[†] Benjamin L. Frankamp,[†] Oktay Uzun,[†] Mark T. Tuominen,[‡] and Vincent M. Rotello*[,†]

Departments of Chemistry and Physics, University of Massachusetts, Amherst, Massachusetts 01003

Received March 12, 2004. Revised Manuscript Received June 1, 2004

Polymer-mediated "bricks-and-mortar" self-assembly of γ-Fe_2O_3 nanoparticles allows modulation of the structure and magnetic properties of the resulting nanoparticle assemblies. Noncovalent assembly of thymine-functionalized nanoparticles using diaminotriazine-functionalized polystyrene provides extended aggregates featuring enhanced ordering relative to control samples of unassembled particles. In addition, the polymer-assembled aggregates feature increased interparticle spacing arising from the polymer "mortar". The enhanced ordering and increased spacing provided by the polymer-mediated assembly alters the strength of interparticle coupling, as manifested by characteristic changes in the magnetic properties of the assemblies.

Magnetic nanoparticles provide a means for constructing pragmatic systems, including high-density data storage arrays[1] and giant magnetoresistance devices.[2] The recent development of preparatory methods that provide nanoparticles featuring high degrees of crystallinity, narrow size dispersions,[3] and unique shapes[4] greatly extend the potential applications of these materials.

Self-assembly of nanoparticle "building blocks" into nanocomposites provides a direct pathway for the incorporation of their unique physical properties into functional materials.[5,6] Several groups have used extremely monodisperse nanoparticles to create beautifully patterned two-dimensional assemblies through controlled evaporation.[7] Expanding on this two-dimensional work, Murray and co-workers recently reported an electrostatically driven layer-by-layer (LBL) assembly of monodisperse nanoparticles using polymers to space each successive layer,[8] while Pileni has prepared three-dimensional assemblies by the evaporation of nanoparticle solutions in applied magnetic fields.[9] These methods create structured assemblies but are generally limited to close packed morphologies. Furthermore, they do not directly address the issue of interparticle spacing, a key factor in tuning the collective properties of nanometer-sized magnets.

Particles separated by a large distance can be considered noninteracting and the resultant magnetic properties are based solely on the physical characteristics of the particles (e.g., volume, crystallinity, etc.). As particles are forced together, either through precipitation or self-assembly, they exhibit a more collective behavior due to magnetic coupling.[10] Magnetic coupling between adjacent particles alters the magnetic properties of a material through magnetostatic interactions.[11] Dipolar coupling between magnetic particles is a specific type of magnetostatic interaction and has been studied by statistically diluting a sample of particles in a known volume.[12] While these studies allow us to investigate the correlation between the interparticle spacing and magnetic properties, they do not provide a mechanism to create a more ordered system.[13]

* To whom correspondence should be addressed. rotello@chem.umass.edu

[†] Department of Chemistry.

[‡] Department of Physics.

(1) Yu, M.; Liu, Y.; Moser, A.; Weller, D.; Sellmyer, D. J. *Appl. Phys. Lett.* **1999**, *75*, 3992−3994.

(2) Kechrakos D.; Trohidou, K. N.; Blackman, J. A. *Phys. Rev. B* **2001**, *63*, 134422.

(3) Hyeon, T. *Chem. Commun.* **2003**, *8*, 927−934.

(4) (a) Puntes, V. F.; Zanchet, D.; Erdonmez, C. K.; Alivisatos, A. P. *J. Am. Chem. Soc.* **2002**, *124*, 12874−12880. (b) Dumestre, F.; Chaudret, B.; Amiens, C.; Fromen, M. C.; Casanove, M. J.; Renaud, P.; Zurcher, P. *Angew. Chem. Int. Ed.* **2002**, *41*, 4286−4289.

(5) (a) Murray, C. B.; Kagan, C. R.; Bawendi, M. G. *Annu. Rev. Mater. Sci.* **2000**, *30*, 545−610. (b) Tripp, S. L.: Pusztay, S. V.; Ribbe, A. E.; Wei, A. *J. Am. Chem. Soc.* **2002**, *124*, 7914−7915.

(6) Crooks, R. M.; Zhao, M.; Sun, L.; Chechik, V.; Yeung, L. K. *Acc. Chem. Res.* **2001**, *34*, 181−190.

(7) (a) Sun, S. H.; Murray, C. B.; Weller, D.; Folks, L.; Moser, A. *Science* **2000**, *287*, 1989−1992. (b) Murray, C. B.; Sun, S. H.; Betley, T. *MRS Bull.* **2001**, *26*, 985−991. (c) Kolny, J.; Kornowski, A.; Weller, H. *Nano Lett.* **2002**, *4*, 361−364 (d) Maye, M. M.; Luo, J.; Lim S., II; Han, L.; Kariuki, N. N.; Rabinovich, D.; Liu, T. B.; Zhong, C. J. *J. Am. Chem. Soc.* **2003**, *125*, 9906−9907.

(8) Sun, S.; Anders, S.; Hamann, H. F.; Thiele, J.-U.; Baglin, J. E. E.; Thomson, T.; Fullerton, E. E.; Murray, C. B.; Terris, B. D. *J. Am. Chem. Soc.* **2002**, *124*, 2884−2885.

(9) (a) Pileni, M. P. *J. Phys. Chem. B* **2001**, *105*, 3358−3371. (b) Pileni, M. P. *Adv. Funct. Mater.* **2001**, *11*, 323−336.

(10) (a) El-Hilo, M.; O'Grady, K.; Chantrell, R. W. *J. Magn. Magn. Mater.* **1992**, *114*, 295−306. (b) Jonsson, T.; Nordblad, P.; Svedlindh, P. *Phys. Rev. B* **1998**, *57*, 497−504.

(11) Exchange coupling is another type of interaction; however, the monolayer present on the above-mentioned nanoparticles greatly reduces its occurrence.

(12) Held, G. A.; Grinstein, G.; Doyle, H.; Sun, S.; Murray, C. B. *Phys. Rev. B* **2001**, *64*.

(13) (a) Poddar, P.; Telem-Shafir, T.; Fried, T.; Marcovich, G. *Phys. Rev. B* **2002**, *66*. (b) Tartaj, P.; Gonzales-Carreno, T.; Serna, C. J. *J. Phys. Chem B* **2003**, *107*, 20−24.

10.1021/cm0495865 CCC: $27.50
Published on Web 07/30/2004

Scheme 1. Polymer Mediated Assembly of Iron Oxide Nanoparticles in (a) the Forced Precipitation of MPC 1 with Hexanes Results in Poorly Ordered Nanoparticles Separated Only by Their Monolayer; (b) Polymer Assembly Effects an Increase in Average Interparticle Spacing and a Qualitative Increase in Overall System Ordering

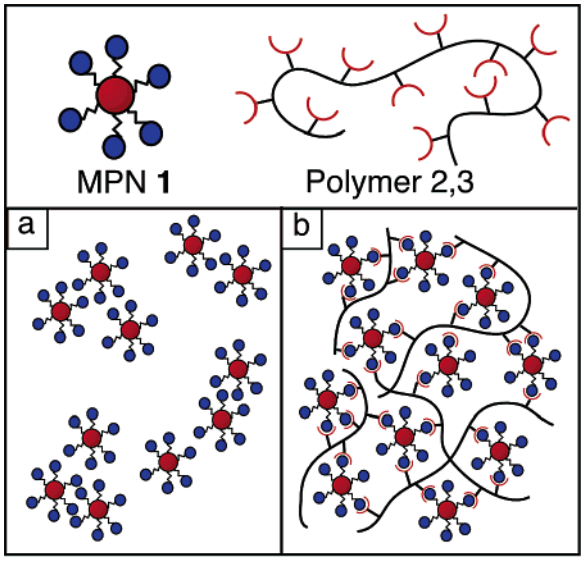

In previous studies using gold nanoparticles, we have shown that polymers functionalized with recognition elements can be used to assemble nanoparticles featuring complementary monolayers, providing increased ordering and interparticle spacing.[14,15] Inserting a magnetic nanoparticle in place of the gold particle would provide a means to investigate the change in bulk magnetic properties as a function of both order and spacing, addressing the difficulties of the aforementioned studies. With use of our recently reported exchange method,[16] the proper functionality can be placed in the monolayer of a magnetic nanoparticle, allowing us to adapt the "bricks and mortar" assembly method to create magnetic assemblies (Scheme 1). Here, we report the use of polymer-mediated self-assembly to modulate both the physical and functional properties of γ-Fe_2O_3 nanoparticles aggregates.[17,18]

Results and Discussion

Thymine-functionalized monolayer-protected nanoparticle (MPN **1**) and triazine-functionalized polymers

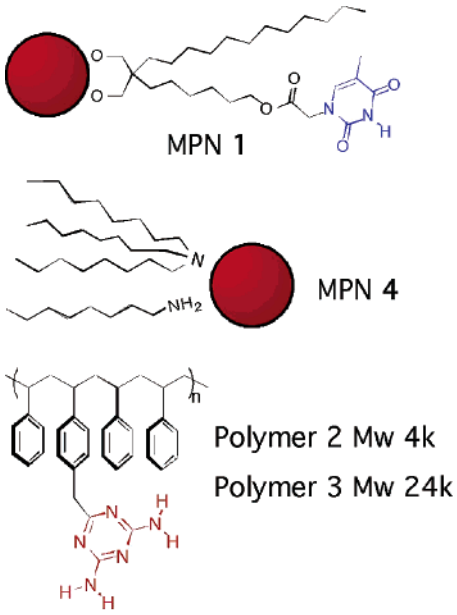

Figure 1. Structure of the components used in this "bricks and mortar" assembly.

2 and **3** (Figure 1) were synthesized as components for "bricks and mortar" self-assembly. The polymer component of the assembly is comprised of varying lengths of poly(styrene-*co*-4-chloromethylstyrene) featuring a styrene/chloromethylstyrene ratio of 3:1. This polymer was synthesized using AIBN-initiated free radical polymerization. Reaction with NaCN followed by dicyandiamide/KOH provided the triazine-functionalized polymer **2** and **3** following previously reported procedures.[19] MPN **1** was prepared from ~6.5-nm-diameter γ-Fe_2O_3 nanoparticles synthesized using Alivisatos' iron Cupferron method.[20] A functional monolayer was installed using a thymine-functionalized diol ligand. In our previous paper describing the place exchange of diol ligands we found that IR spectroscopy was an excellent method for characterization of the monolayer during the exchange process. Of particular utility is the emergence of the N−H (~3400 cm^{-1}) and C═O stretches (1680 cm^{-1}) and the increased absorbance at ~1050 cm^{-1} from the C−O stretch (Figure 2).

Mixing solutions of MPN **1** with polymers **2** and **3** in 1:1 chloroform/tetrahydrofuran gave turbid solutions followed by complete precipitation after 24 h. Solutions made from the addition of polymer **2** to solutions of iron oxide nanoparticles MPN **4** remained homogeneous, verifying that the assembly process is driven by specific molecular recognition interactions between MPN **1** and

(14) (a) Boal, A. K.; Ilhan, F.; DeRouchey, J. E.; Thurn-Albrecht, T.; Russell, T. P.; Rotello, V. M. *Nature* **2000**, *404*, 746−748. (b) Boal, A. K.; Galow, T. H.; Ilhan, F.; Rotello, V. M. *Adv. Funct. Mater.* **2001**, *11*, 461−467. (c) Boal, A. K.; Gray, M.; Ilhan, F.; Clavier, G. M.; Kapitzky, L.; Rotello, V. M. *Tetrahedron* **2002**, *58*, 756−770. (d) Frankamp, B. L.; Uzun, O.; Ilhan, F.; Boal, A. K.; Rotello, V. M. *J. Am. Chem. Soc.* **2002**, *124*, 892−893.

(15) For other examples of molecular-recognition-based assembly of nanoparticles, see: (a) Mirkin, C. A.; Letsinger, R. L.; Mucic, R. C.; Storhoff, J. J. *Nature* **1996**, *382*, 607−609. (b) Alivisatos, A. P.; Johnsson, K. P.; Peng, X. G.; Wilson, T. E.; Loweth, C. J.; Bruches, M. P.; Schultz, P. G. *Nature* **1996**, *382*, 609−611. (c) Schmid, G.; Chi, L. F. *Adv. Mater.* **1998**, *10*, 515−526. (d) Aherne, D.; Rao, S. N.; Fitzmaurice, D. *J. Phys. Chem. B* **1999**, *103*, 1821−1825. (e) Liu, J.; Mendoza, S.; Roman, E.; Lynn, M. J.; Xu, R. J.; Kaifer, A. E. *J. Am. Chem. Soc.* **1999**, *121*, 4304−4305.

(16) Boal, A. K.; Das, K.; Gray, M.; Rotello, V. M. *Chem. Mater.* **2002**, *14*, 2628−2636.

(17) For the self-assembly of Fe_3O_4 nanoparticles directed by intermonolayer interactions, see: Jin, J.; Iyoda, T.; Cao, C. S.; Song, Y. L.; Jiang, L.; Li, T. J.; Zhu, D. B. *Angew. Chem., Int. Ed.* **2001**, *40*, 2135−2138.

(18) For examples of polymer/magnetic nanoparticle composite materials, see: (a) Kommareddi, N. S.; Tata, M.; John, V. T.; McPherson, G. L.; Herman, M. F.; Lee, Y.-S.; O'Connor, C. J.; Akkara, J. A.; Kaplan, D. L. *Chem. Mater.* **1996**, *8*, 801−809. (b) Ely, T. O.; Amiens, C.; Chaudret, B.; Snoeck, E.; Verelst, M.; Respaud, M.; Broto, J.-M. *Chem. Mater.* **1999**, *11*, 526−529. (c) Tang, B. Z.; Geng, Y.; Lam, J. W. Y.; Li, B.; Jing, X.; Wang, X.; Wang, F.; Pakhomov, A. B.; Zhang, X. X. *Chem. Mater.* **1999**, *11*, 1581−1589. (d) Dresco, P. A.; Zaitsev, V. S.; Gambino, R. J.; Chu, B. *Langmuir* **1999**, *15*, 1945−1951. (e) Ginzburg, M.; MacLachlan, M. J.; Yang, S. M.; Coombs, N.; Coyle, T. W.; Raju, N. P.; Greedan, J. E.; Herber, R. H.; Ozin, G. A.; Manners, I. *J. Am. Chem. Soc.* **2002**, *124*, 2625−2639.

(19) , (a) Hawker, C. J. *J. Am. Chem. Soc.* **1994**, *116*, 11185−11186. (b) Harth, E.; Hawker, C. J.; Fan. W.; Waymouth, R. M. *Macromolecules* **2001**, *34*, 3856−3862.

(20) Rockenberger, J.; Scher, E.; Alivisatos, A. P. *J. Am. Chem. Soc.* **1999**, *121*, 11595−11596.

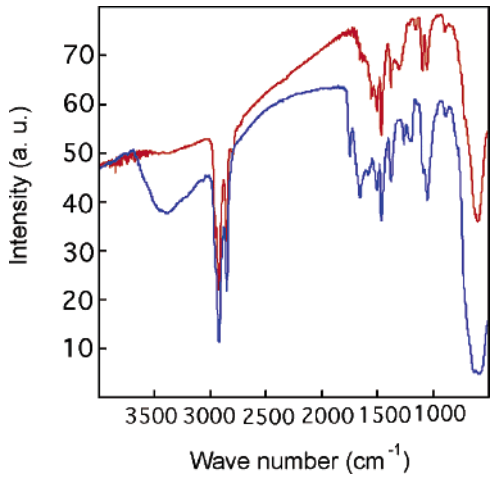

Figure 2. IR of the as-prepared amine-covered MPN **4** (in red) and the post-functionalized MPN **1** (in blue).

polymer **2**. A control sample of closely packed particles was prepared by precipitating MPN **1** from solution with hexanes, providing nanoparticles spaced only by the monolayer.

Small-angle X-ray scattering (SAXS) was used to analyze the structural characteristics of our nanoparticle assemblies. With hexanes-precipitated MPN **1**, a center-to-center particle spacing of 6.8 nm was observed (Figure 3), in good agreement with particles spaced only by their monolayer.[21] When polymer **2** was used to assemble MPN **1**, the interparticle spacing increased to 7.6 nm. This increase is consistent with the assembly motif shown in Scheme 1, where a polymer chain separates the nanoparticles in the assemblies.[22,23] The increase in spacing due to polymer assembly of MPN **1** was found to be slightly smaller (0.8 nm) than the same distance previously observed for polymer-assembled gold nanoparticles (1.4 nm). This is likely due to the sparsely packed nature of the monolayer on the γ-Fe_2O_3 nanoparticles[16] and the large increase in nanoparticle core size relative to the polymer backbone. As expected, near-identical behavior was observed with higher molecular weight polymer **3**, indicating that the length of the polymer does not dictate interparticle spacing.[24] SAXS provides quantitative information concerning the interparticle spacing as well as information regarding overall system ordering. In our studies, the precipitated sample generates a SAXS peak that is significantly broader that that of the polymer-assembled samples, indicating a much larger distribution of interparticle spacing (i.e., more disorder). Concurrently, there is a marked increase in peak intensity for the polymer-assembled sample, diagnostic of increased ordering and more uniform particle distribution.[14] The combination of increased ordering and interparticle spacing provided by our "bricks and mortar" method should result in modulated magnetic behavior.

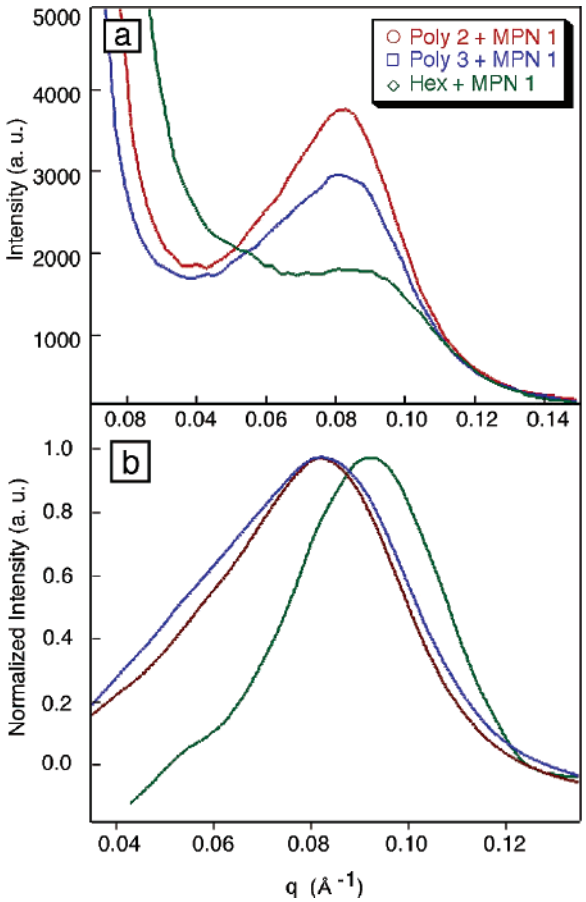

Figure 3. (a) SAXS profiles for MPN **1** (green) precipitated with hexanes and assembled with polymer **2** (red) and polymer **3** (blue). (b) Background subtracted and normalized plot demonstrating the decrease in q as MPN **1** is assembled with polymers **2** and **3**.

Magnetic Characterization

A superconducting quantum interference device (SQUID) was used to acquire zero-field-cooled (ZFC), field-cooled (FC), and field-dependent magnetization measurements for the precipitated and assembled samples of MPN **1**. MPN **1** consists of 6.5-nm γ-Fe_2O_3 nanoparticles that are superparamagnetic at room temperature,[25] becoming ferromagnetic at low temperatures. The superparamagnetic−faramagnetic transition occurs at the blocking temperature[26] (T_B), which is not unique but depends weakly on the time scale of experimental measurement.[27] The T_B of a sample can be obtained through a ZFC/FC scan that sweeps a chosen temperature range while recording the magnetic response of your sample to a constant applied field.[28] The control sample of precipitated particles showed a

(21) The q value of maximum intensity was converted to distance through the relationship $q = 2\pi/d$ where d is in values of Å.

(22) Upon assembly the SAXS plot sharpens considerably qualitatively, indicating a more ordered assembly. This observation is consistent with the earlier MPC study and the blocking temperature data.

(23) Martin, J. E.: Wilcoxon, J. P.; Odinek, J.; Provencio, P. *J Phys. Chem. B* **2000**, *104*, 9475−9486.

(24) A 14K molecular weight polymer showed consistently erratic spacing and magnetic values throughout the study and that data is not shown. The origin of this discrepancy is unclear at this time.

(25) In the superparamagnetic state the thermal energy k_BT is large enough to overcome the energy barrier for magnetization reversal and produce rapid fluctuations that lead to a time-averaged magnetization of zero-termed superparamagnetic relaxation.

(26) In the case of noninteracting particles the energy barrier K_1V is determined by the intrinsic anisotropy energy density and the volume of the nanoparticle. $T_B \sim K_1V/30k$ serves as a practical definition of blocking temperature for a measurement time of ~1000 s.

(27) Dimitrov, D. A.; Wysin, G. M. *Phys. Rev. B* **1996**, *54*, 9237.

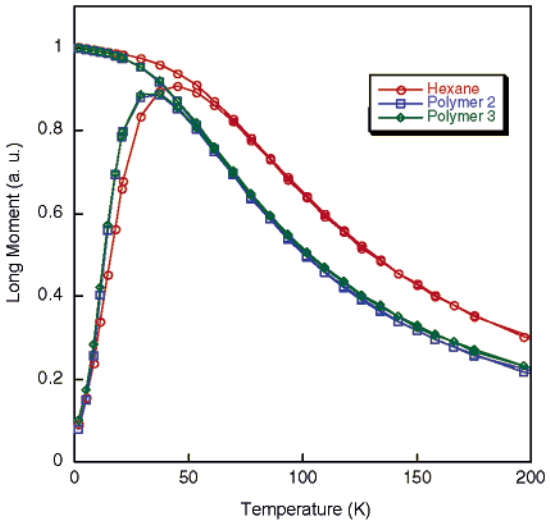

Figure 4. FC and ZFC magnetization plots for MPN **1** precipitated with hexanes and assembled with polymer **2** and polymer **3**.

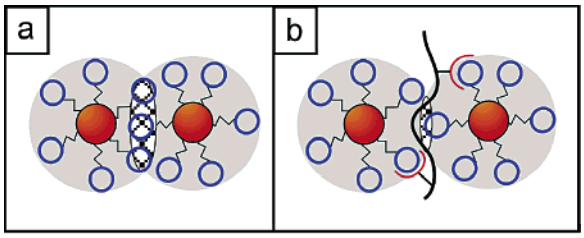

Figure 5. Schematic representation of the interparticle magnetic field interactions. The checked area in (a) represents the effective magnetic coupling that is decreased upon assembly with the polymer (b).

T_B of 47 K while the assembled samples both showed a T_B of 37 K (Figure 4). This change in blocking temperature can be explained by a decrease in dipolar coupling arising from the increased interparticle spacing.

The T_B of magnetic nanoparticles is directly related to its volume.[29] Our samples were obtained from the *exact same batch* of nanoparticles, thus eliminating core size discrepancies. The observed decrease of T_B is therefore a direct consequence of the polymer-controlled increased in spacing, as schematically depicted in Figure 5. As the particles are assembled by the polymer, the dipolar coupling between particles should decrease, resulting in an "effective" volume decrease verses the control sample.

Interestingly, the ZFC plot for the assembled samples are sharper than the control sample, mirroring the change observed in the SAXS. The width of the ZFC plot is a representation of the distribution of spin alignment and the observed sharpening could easily be explained in terms of increased ordering. These complimentary observations suggest a correlation between the increased SAXS intensity, indicative of a more ordered system, and the sharper T_B plot that is caused by a more uniform distribution of interacting dipoles.

(28) During the ZFC process, the samples were cooled from 298 to 1.8 K, "blocking" the random magnetic order, resulting in net magnetization of zero at the outset of the experiment. A small field was applied, 100 Oe, and the magnetic moment measured as a function of temperature.

(29) Vestal, C. R.; Zhang, J. Z. *Chem. Mater.* **2002**, *14*, 3817−3822.

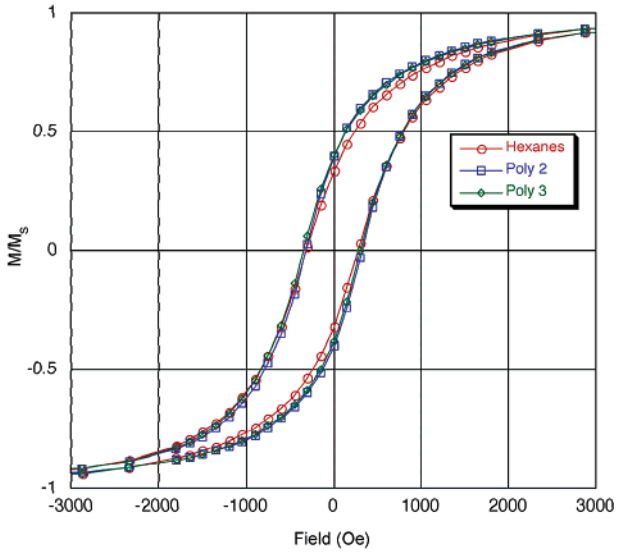

Figure 6. Field sweep hysteresis plot of MPC **1** precipitated with hexanes and assembled with polymers **2** and **3**. Plots are normalized to saturation magnetization.

To further investigate the effect of polymer assembly and spacing, field-dependent magnetization studies were obtained on films of MPN **1** combined with polymers **2** and **3** and the hexane control.[30] Hysteresis plots offer a view into the collective behavior of nanoparticle systems, providing values of remanence (M_R), coercivity (H_C), and saturation magnetization (M_S). At low temperature hysteretic behavior was observed in all cases and the plots are shown in Figure 6. The remanent magnetization factor for the hexane control is 0.34 emu while the polymer-assembled samples show slightly higher values of 0.40 emu. The coercivity of the assembled particles was found to be ∼332 Oe while the hexane control showed a smaller value of 300 Oe (Table 1).[31]

Again, since we used the same batch of nanoparticles, the only reasonable explanation for the change in coercivity and remanence is the polymer assembly. It is known that the coercivity of a superparamagnetic nanoparticle is inversely related to the particle size.[29] The "effective" volume overlap between the particles is lower in the polymer-assembled samples, resulting in an increase in the coercivity relative to the more highly coupled, effectively larger, particles in the hexane control. Likewise, the increase in remanence of the polymer-assembled films arises from the decrease in dipolar coupling between the particles. In the hexanes-precipitated aggregate, the stronger coupling lowers the remanence by inducing a greater degree of frustration in the sample.[12] Additionally, the competition between interparticle anisotropy and spin relaxation increases with dipolar coupling.[32]

In summary, we have demonstrated the use of polymer-mediated "bricks-and-mortar" assembly to alter the magnetic properties of γ-Fe_2O_3 nanoparticle ensembles.

(30) Field sweep measurements were made at 1.8 K between 20000 and −20000 Oe and back.

(31) These values are in good agreement with a recent report from Cerna and co-workers who reported a value of 351 Oe for a γ-Fe_2O_3 particle of similar size. Tartaj, P.; Gonzales-Carreno, T.; Serna, C. J. *J. Phys. Chem. B* **2003**, *107*, 20−24.

(32) For a more detailed explanation of the effect of interparticle distance on M_R, see ref 12 and citations therein.

Table 1. Summary of Structural and Functional Change upon Polymer-Mediated Assembly

	polymer (M_w)	spacing (nm)	blocking temp. (K)	reduced rem. (emu)	coercivity (Oe)
hex + MPC **1**		6.8	47	0.34	300
poly **2** + MPC **1**	4000	7.6	37	0.40	332
poly **3** + MPC **1**	24000	7.6	37	0.40	332

This assembly process increases particle spacing and system order demonstrated by a shift to lower q values and overall peak sharpening in the SAXS spectrum of the polymer-assembled samples. This structural modulation results in a decrease in T_B and increases in remanence and coercivity. The observed modulation in the bulk magnetic properties is based solely on polymer-mediated self-assembly, providing a means to alter the output of magnetic nanoparticle-based materials. We are currently exploring applications for this methodology and will report our findings in due course.

Experimental Section

Chemicals. THF was distilled from Na:benzophenone under argon and anhydrous ether was purchased in sealed cans from VWR. All reactions were carried out in oven-dried glassware under an atmosphere of argon. ^{1}H NMR spectra were recorded in $CDCl_3$ (purchased from Cambridge Isotope Labs, Inc.) at 200 MHz and referenced internally to TMS at 0.0 ppm. IR spectra were recorded on Midac M1200. All reagents and other solvents were used as received from commercial sources.

Preparation of Nanoparticle Assemblies. All nanoparticle assemblies were prepared from the same batch of MPN 1, and the same samples were used for TEM, SAXS, and SQUID analysis. For the polymer assembly, 2 mg/mL solutions of polymers **2**−**3** in 1:4 THF:$CHCl_3$ and a ∼5 mg/mL solution of MPNs **1** and **4** in $CHCl_3$ were used. Equal volumes of the polymer and nanoparticle solutions were mixed, and turbidity was observed almost immediately, with TEM samples withdrawn after 1 h. After 24 h, precipitation was complete, and the solid was washed extensively with $CHCl_3$ and then dried overnight before being subjected to either SAXS or SQUID. For the hexanes-precipitated sample, 1 mL of the MPN **1** solution at 5 mg/mL was combined with 10 mL of hexanes. A TEM sample was withdrawn after 10 min, and precipitation was complete in about 3 h. The mother liquor was removed and the solid treated as above.

Characterization of Nanoparticle Assemblies. *Transmission Electron Microscopy.* A drop of the turbid solutions was placed on a 300-mesh Cu grid covered with a carbon film. The samples were then examined on either a JEOL 100CX or a JEOL 200 operating at 100-keV TEM.

Small Angle X-ray Scattering. To prepare samples for SAXS, ∼1 mL of the turbid solutions was withdrawn from the main solution and transferred to a vial containing a 1-cm^2 piece of Mylar on the bottom. Precipitation was allowed to go to completion, and the precipitate was deposited on the Mylar. The mother liquor was removed and the sample washed with $CHCl_3$ and then dried. Spectra were acquired on a molecular metrology instrument producing an X-ray λ of 0.154 Å. The scattering intensity is presented as a function of the wave vector $q = (4\pi/\lambda)\sin(2\theta/2)$ where 2θ is the scattering angle and λ the X-ray wavelength. The background subtraction was carried out identically to that in ref 33.

SQUID. Data were acquired on a QuantumDesign MPMS 7 SQUID Magnetometer. ZFC−FC plots were acquired by cooling the sample to 1.8 K in the absence of a magnetic field, and then a field of 100 Oe was applied and the sample slowly warmed to 300 K and returned to 1.8 K, thus acquiring FC and ZFC plots in a single temperature sweep. Field sweep measurements were taken at a temperature of 1.8 K, sweeping from 20000 to −20000 Oe and back. Blocking temperature assignments were made by fitting the ZFC plot to a Gaussian curve using Igor software.

Acknowledgment. This research was supported by the National Science Foundation: CHE-0213354 and CHE-0304173 (V.M.R.) DMI-0103024 (MT) and MRSEC instrumentation. We thank David Shultz (NCSU) for assistance with preliminary SQUID data. B.L.F. acknowledges the ACS Division of Organic Chemistry Graduate Fellowship sponsored by the Procter and Gamble Company.

Supporting Information Available: Polymer synthesis follows ref 14. NMR, GPC, and synthetic schemes and details can be found in the Supporting Information along with X-ray diffraction results of the as-prepared nanoparticles and TEM of the resulting aggregates.

CM0495865

(33) Frankamp, B. L.; Boal, A. K.; Rotello, V. M. *J. Am. Chem. Soc.* **2002**, *124*, 15146−15147.